



Enantiomeric recognition of α -(1-naphthyl)ethylammonium perchlorate by enantiomerically pure dimethylphenazino-18-crown-6 ligand in solid and gas phases

Tímea Gérczei,^a Zsolt Böcskei,^a György M. Keserű,^b Erika Samu^c and Péter Huszthy^{d,*}

^aDepartment of Theoretical Chemistry, Lorand Eötvös University, H-1521 Budapest, Hungary

^bDepartment of Chemical Information Technology, Technical University of Budapest, H-1521 Budapest, Hungary

^cInstitute for Organic Chemistry, Technical University of Budapest, H-1521 Budapest, Hungary

^dResearch Group for Alkaloid Chemistry, Hungarian Academy of Sciences, H-1521 Budapest, Hungary

Received 28 April 1999; accepted 20 May 1999

Abstract

X-Ray crystallographic studies of enantiomerically pure dimethylphenazino-18-crown-6 ligand (*R,R*)-**1** and its complexes with the enantiomers of α -(1-naphthyl)ethylammonium perchlorate NapEt were carried out. These studies clearly show that the heterochiral complex (*R,R*)-**1**-(*S*)-NapEt is more stable than the homochiral one (*R,R*)-**1**-(*R*)-NapEt. It was pointed out that besides the hydrogen bonding, mainly the π - π interaction between the aromatic systems of the host and guest, and the difference in steric repulsions were responsible for enantioselectivity. Molecular mechanical calculations using the LMOD/MINTA method also predicted the heterochiral complex to be more stable than the homochiral one in the gas phase. © 1999 Elsevier Science Ltd. All rights reserved.

1. Introduction

Enantiomeric recognition, as a special case of molecular recognition, involves the discrimination between the enantiomers of a molecule by an optically active chiral receptor. This phenomenon, which is very important in nature, can also be engineered into relatively simple synthetic molecules. Among synthetic receptors which bind molecules enantioselectively, chiral crown ethers have attracted considerable attention, because they are not only suitable models in helping to increase understanding of enantiomeric recognition in nature, but they also have many applications in organic, pharmaceutical, biological and analytical chemistry.¹

Over the last quarter of a century a wide range of chiral crown ethers has been prepared in attempts to enhance their discrimination between the enantiomers of different molecules. Among them a number

* Corresponding author. E-mail: huszthy.szk@chem.bme.hu

of chiral crown ethers have been prepared containing pyridine,² pyrimidine³ and phenanthroline⁴ units. These enantiomerically pure chiral ligands and their discrimination between the enantiomers of organic ammonium salts have been extensively studied.^{2–6}

Very recently we described the preparation of enantiomerically pure dimethyl-substituted phenazino-18-crown-6 ligand (*R,R*)-**1** (Fig. 1) as the first representative of a chiral crown ether containing phenazine unit.⁷

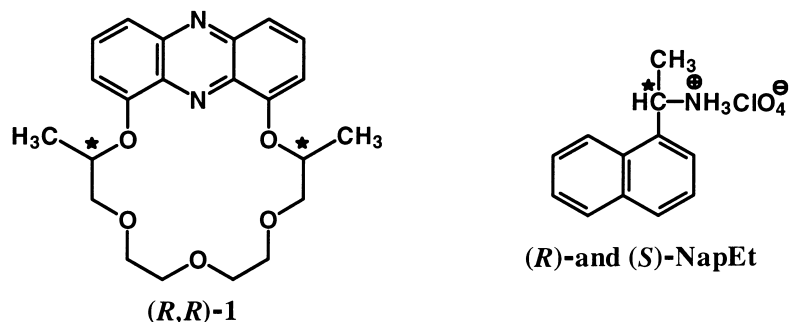


Figure 1. Chemical formulas of the host (*R,R*)-**1** and guest NapEt molecules

Ligand (*R,R*)-**1** has a tricyclic ring system which imparts high rigidity to the upper part of the molecule, i.e. close to the stereogenic centers. Also the extended π -system of the phenazine ring provides a stronger π - π interaction with an organic ammonium salt containing an aromatic moiety. Both features assist enantioselectivity.^{4–6} For the first step to study enantiomeric recognition we have prepared suitable crystals of the free ligand (*R,R*)-**1** and also its complexes with both enantiomers of α -(1-naphthyl)ethylammonium perchlorate NapEt using the same solvent. Beside reporting the results of X-ray studies, we also disclose here our molecular mechanical calculations which provide support that the stability order observed in solid state stands in the gas phase too.

2. Results and discussion

Crystal structures of macrocyclic host (*R,R*)-**1** in its uncomplexed form as well as in its complexes with (*R*)- and (*S*)-NapEt as guests have been established. The three structures constitute a rarely found systematic series. The structures provide grounds for the interpretation of the chiral recognition process effected by the host and the guest. ORTEP drawings of the three structures with atomic numberings are shown in Fig. 2 [(*R,R*)-**1**], Fig. 3 [(*R,R*)-**1**-(*R*)-NapEt complex] and Fig. 4 [(*R,R*)-**1**-(*S*)-NapEt complex].

Although in the homochiral complex (*R,R*)-**1**-(*R*)-NapEt there are two molecules in the asymmetric unit, they have very similar conformations (r.m.s.d.=0.306 Å for the nonhydrogen atoms) and therefore we only present molecule A in Fig. 3.

It is a common feature of the structures that some of the atoms of the ligand (*R,R*)-**1** that are further away from the phenazine ring show a fairly strong thermal motion. In the uncomplexed form there is a relatively large disordered segment (from C4A to O8A atoms) which is reduced to two atoms (C6A and C7A) in one of the two crystallographically independent molecules of the asymmetric unit of the homochiral (*R,R*)-**1**-(*R*)-NapEt complex.

On the other hand in the more stable heterochiral (*R,R*)-**1**-(*S*)-NapEt complex no static disorder was observed, probably due to a more extensive hydrogen bonding network between the host and guest molecules (Fig. 4).

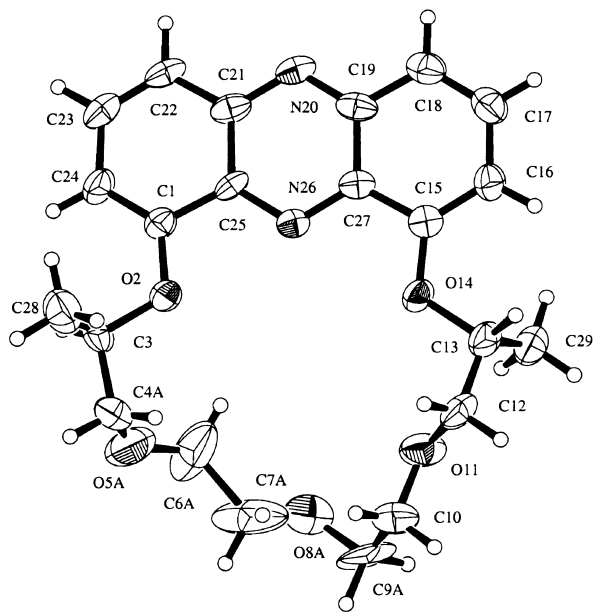


Figure 2. An ORTEP drawing of the structure of (R,R) -1 in its uncomplexed form as found in its crystal

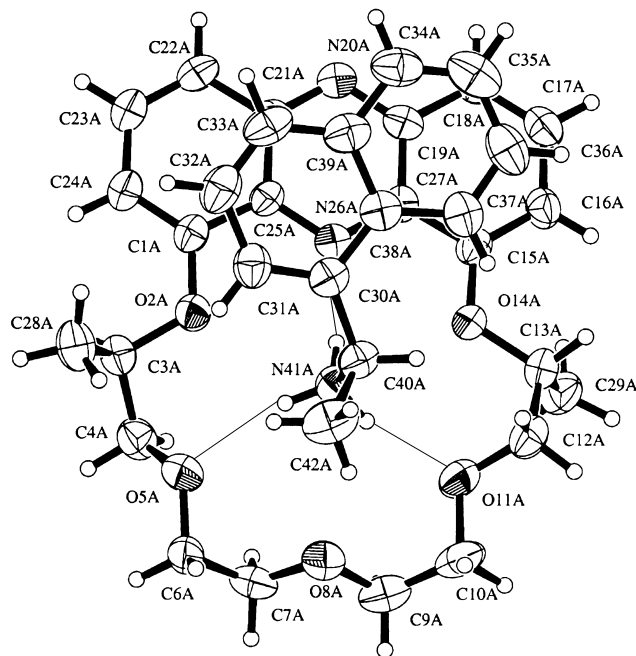


Figure 3. An ORTEP drawing of the structure of homochiral complex (R,R) -1-(R)-NapEt as found in its crystal

In the latter complex we also identified a water molecule hydrogen-bonded to an oxygen of a neighbouring perchlorate anion. The host–guest complexes are held together on the one hand by a strong system of hydrogen bonds between the three protons of the ammonium ion as well as the nitrogen and two alternate oxygen atoms of the crown ether, and on the other hand by π – π interactions between the aromatic rings of (R,R) -1 and NapEt (Table 1, Figs. 3 and 4).

As shown in Table 1 the strengths of the hydrogen bonds (as characterized by the bridgehead atom

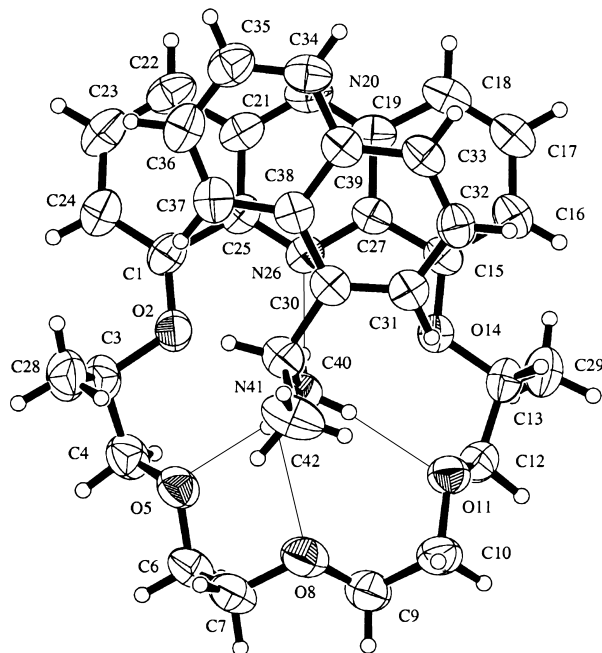


Figure 4. An ORTEP drawing of the structure of heterochiral complex (R,R) -**1**– (S) -NapEt as found in its crystal

Table 1
The bridgehead atom distances and hydrogen bond angles

	(R,R) - 1 – (R) -NapEt (A)		(R,R) - 1 – (R) -NapEt(B)		(R,R) - 1 – (S) -NapEt	
	dist./Å	Angle/deg	dist./Å	angle/deg	Dist./Å	angle/deg
N41 - N26	2.942 (7)	173 (4)	2.964 (7)	166 (4)	2.932 (5)	166 (1)
N41 - O5	3.011 (7)	161 (2)	2.916 (8)	165 (3)	2.951 (5)	163 (3)
N41 - O8	-	-	-	-	2.902 (5)	116 (2)
N41 - O11	2.887 (7)	164 (5)	2.911 (7)	165 (3)	2.961 (5)	167 (1)

distances and the H-bond angles) are not significantly different in the two complexes even though in the more stable heterochiral complex we can find a bifurcated hydrogen bond instead of a normal one (Fig. 4).

Since in the latter complex (S) -NapEt is fixed to the crown ether (R,R) -**1** at four positions, this bifurcated hydrogen bond could play a role in the higher rigidity of the crown ether part opposite to the phenazine ring. In our view, most of the difference in stability of the two diastereomeric complexes is attributed to the attractive π – π interaction of the naphthalene and phenazine rings as well as to the repulsive interaction between certain hydrogens of NapEt and the methyl substituents of (R,R) -**1**.

There is a relatively small difference in the mean distances between the naphthalene and phenazine ring atoms in the two complexes. On the other hand the interplanar angle between the naphthalene and phenazine rings is around 14.5 degrees in both crystallographically independent molecules of the less stable homochiral complex, while in the more stable heterochiral complex the two planes are much more parallel as indicated by the value of the corresponding angle (7.3 degrees) (Table 2, Figs. 5 and 6).

So the interplanar angle between the two aromatic ring systems is smaller in the heterochiral complex than in the homochiral one, corresponding to a tighter fit and a stronger (more extensive) π – π interaction in the former case. In the case of the complexes of (R) - and (S) -NapEt with $(4S,14S)$ –(–)-4,14-dimethyl-3,6,9,12,15-pentaoxa-21-azabicyclo[15.3.1]heneicosa-1(21),17,19-triene-2,16-dione, fur-

Table 2

The most striking carbon and hydrogen short contacts between atoms of (*R,R*)-1 and NapEt. The distances of naphthalene ring centroids from those of the phenazine ring and the interplanar angles between the two rings

		(<i>R,R</i>)-1-(<i>R</i>)-NapEt(A)	(<i>R,R</i>)-1-(<i>R</i>)-NapEt(B)	(<i>R,R</i>)-1-(<i>S</i>)-NapEt
		(Å)	(Å)	(Å)
C28	H31	3.13 (1)	3.26 (1)	6.64 (1)
	H32	3.79 (1)	3.62 (1)	8.37 (1)
	H36	8.07 (1)	8.82 (1)	5.01 (1)
	H37	7.01 (1)	7.22 (1)	3.57 (1)
	H40	5.92 (1)	6.09 (1)	3.29 (1)
Distance ^a		3.63 (1)	3.67 (1)	3.50 (1)
angle ^b		14.2 ° (2)	14.7° (2)	7.3° (1)

^aThe mean distance between phenazine and naphthalene rings

^bThe interplanar angle between phenazine and naphthalene rings

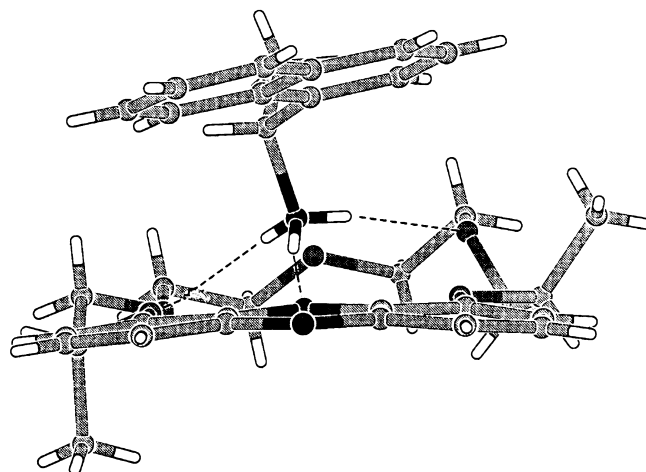


Figure 5. A side view of the complex emphasizing the interplanar angle between the aromatic ring systems in the homochiral complex (*R,R*)-1-(*R*)-NapEt

ther on (*S,S*)-dimethyldiketopyridino-18-crown-6 ligand,^{8,9} the interplanar angles between the naphthalene and pyridine rings are smaller (6.9 degrees) in the homochiral than in the heterochiral (11.9 degrees) complex.⁹ So contrary to our observation, in the latter case the interplanar angle between the aromatic ring systems is greater in the more stable complex than the corresponding angle in the less stable one.

In the case of pyridino-18-crown-6 ligands and organic ammonium salts containing only one benzene ring, there are examples in the literature when π - π interaction is absent^{10,11} or a weak π - π interaction could be observed.¹² When the aromatic system is extended either in the guest or in the host, π - π interaction between ring systems becomes more pronounced.^{4,11} Extending the aromatic system of the guest molecule (e.g. naphthalene ring instead of a benzene ring), the distance between the center of the aromatic rings of the host and the guest is getting smaller. Using the published co-ordinates we found that the (*R,R*)-dimethyldiketopyridino-18-crown-6 ligand complexed with (*R*)-2-hydroxy-1-phenylethylammonium perchlorate, the distance between the centers of the aromatic rings is 3.78 Å,¹² while in the case of (*R*)-NapEt guest this distance is 3.52 Å.^{8,9}

The above comparisons suggest that the more extended the aromatic systems are, the tighter the π - π interaction between the aromatic rings of the host and guest molecules is.

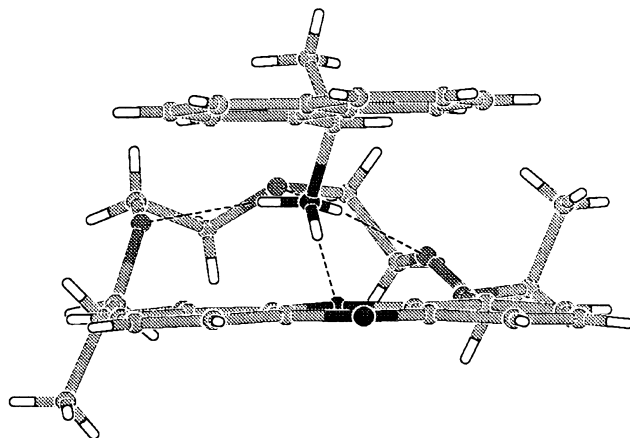


Figure 6. A side view of the complex emphasizing the interplanar angle between the aromatic ring systems in the heterochiral complex (R,R) -**1**– (S) -NapEt

On the basis of this set of structures we conclude that beside the hydrogen bonds mainly π – π interactions are responsible for the relatively fixed mutual positions of the two aromatic systems in complexes (R,R) -**1**– (R) -NapEt and (R,R) -**1**– (S) -NapEt. In addition to the above mentioned attractive forces, repulsive interactions between certain hydrogens of NapEt and the methyl substituents at the stereogenic centers of (R,R) -**1** are also responsible for positioning of the naphthalene moiety above the phenazine ring. In the case of the heterochiral complex the naphthalene ring occupies a relatively distant position from the C28 methyl group. In order to avoid a strong repulsion between the hydrogen atoms of (R) -NapEt and the C28 methyl group of (R,R) -**1** in the homochiral complex, the naphthalene ring must take a position in which it is less parallel to the phenazine moiety (see Table 2 and Figs. 3 and 5). In the case of diastereomeric complexes (R,R) -**1**–NapEt the shortest distance between the closest hydrogen of the guest and the C28 methyl carbon of the host is 3.13 Å in the homochiral complex and 3.29 Å in the heterochiral one. From this analysis it seems that the extension of the aromatic system of the crown ether provides a larger area for π – π interaction which allows the naphthalene ring in the case of (S) -NapEt to assume a position where the repulsive interaction is smaller with the C28 hydrogens. In the case of (S,S) -dimethyldiketopyridino-18-crown-6 ligand complexed with the enantiomers of NapEt, the shortest distances were 3.11 Å for the homochiral complex and 3.33 Å for the heterochiral one.^{8,9}

Comparing the structures of (R,R) -**1** in its complexes to the uncomplexed (R,R) -**1**, we can conclude that the crown ether atoms close to the phenazine ring suffer less conformational changes in the heterochiral complex than the corresponding atoms do in the homochiral one. This feature can be characterized by an r.m.s. deviation of 0.08 Å (heterochiral-uncomplexed) and 0.26 Å (homochiral-uncomplexed) between the macroring portions of (R,R) -**1** close to the phenazine ring (C1, O2, C3, C4, C28, C12, C13, C29, O14, C15). Therefore these parts of (R,R) -**1** must undergo more significant conformational changes to be able to bind the (R) -NapEt guest than the (S) -NapEt one (Fig. 7). In the case of (S,S) -dimethyldiketopyridino-18-crown-6 ligand^{8,9,13} complexed with the enantiomers of NapEt the r.m.s. deviations of the corresponding atoms are 0.10 Å (heterochiral-uncomplexed) and 0.26 Å (homochiral-uncomplexed).¹³ The difference in the r.m.s. deviations reflects a more selective binding of the preferred enantiomer of NapEt by (R,R) -**1** than by the (S,S) -dimethyldiketopyridino-18-crown-6 host, especially if we consider the higher rigidity of the former host compared to the latter one. We firmly believe that the conformational differences of the macroring portions further away from the stereogenic centers and the aromatic rings of the above mentioned two hosts are not so important from an enantioselectivity point of view due to a large number of low energy conformations allowed in those regions.

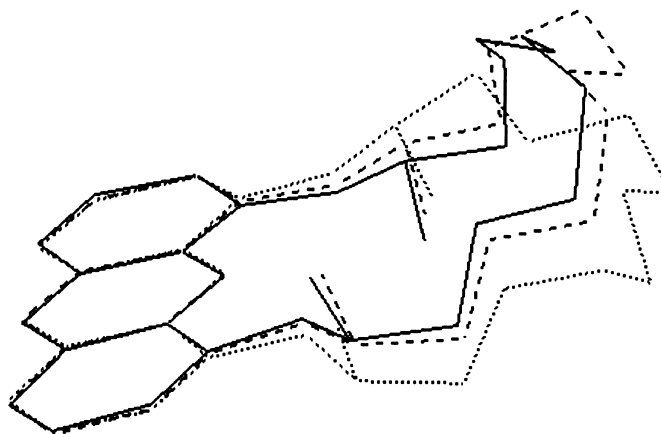


Figure 7. The superposition of the crown ether conformations found in the crystals of (R,R) -**1** (continuous line), (R,R) -**1**– (R) -NapEt (dotted line) and (R,R) -**1**– (S) -NapEt (dashed line)

Molecular modeling can also provide invaluable help to predict binding affinity and rationalize binding geometry, hence contributing to better understanding of chiral recognition. Here we report the successful application of the new LMOD/MINTA computational methodology^{14–16} for the rapid prediction of enantioselectivity of (R,R) -**1** toward (R) - and (S) -NapEt in the gas phase. The LMOD/MINTA method addresses the sampling problem for calculating binding free energies at two different levels. First, a global conformational search is carried out with LMOD¹⁴ to identify the low-energy regions of the potential energy surface (PES), which correspond to the low-energy binding conformations of the complex. Local sampling of each individual conformational energy well is then accomplished by utilizing the mode integration technique^{15,16} with the MINTA program. The LMOD/MINTA procedure was applied here to predict the enantioselectivity observed in the recognition process. The LMOD/MINTA results gave the observed preference and affinity within ~ 32.6 kJ/mol of (R,R) -**1** for binding (S) - and (R) -NapEt. This is in accordance with the interpretation of the comparative X-ray analysis performed on the diastereomeric complexes (R,R) -**1**– (R) -NapEt and (R,R) -**1**– (S) -NapEt. The LMOD searches afforded 12 (R,R) -**1**– (R) -NapEt and 17 (R,R) -**1**– (S) -NapEt complex binding conformations. The gas phase global minimum structures of both diastereomers ($E_{\min} = -26.57$ kJ/mol and $E_{\min} = -0.52$ kJ/mol, for the heterochiral and homochiral complexes, respectively), are in excellent agreement with the X-ray structures (heavy atom superposition r.m.s. is 0.48 Å for the homochiral complex and 0.61 Å for the heterochiral one).

3. Conclusions

We examined the crystal structures of macrocycle (R,R) -**1** in its uncomplexed form as well as in its complexes with (R) - and (S) -NapEt. Based on our studies described here we can draw the following conclusions:

- (i) the interplanar angle between the phenazine ring of the host and the naphthalene moiety of the guest is smaller in the heterochiral than in the homochiral complex corresponding to a tighter π – π interaction in the former case. In order to avoid a strong repulsion between the hydrogen atoms of the guest and the C28 methyl group of the host in the homochiral complex, the naphthalene ring must occupy a position in which it is less parallel to the phenazine moiety;
- (ii) extending the aromatic system of the crown ether host provides a larger area for π – π interactions for the naphthalene ring of the ammonium salt guest, so a tighter association of the complexes

takes place where the difference in steric repulsion becomes more pronounced which can lead to enhanced enantioselectivity;

- (iii) a search in the literature has shown that in the case of the crown ether hosts and organic ammonium salt guests with only a single aromatic ring, the π – π interactions are too weak to keep the aromatic systems right above the plane of each other. However, in the case of crown ether hosts with extended aromatic systems the π – π interactions secure a better overlapping with the naphthalene ring of the NapEt guest;
- (iv) comparing the structures of (*R,R*)-**1** in the complexes to the uncomplexed (*R,R*)-**1** has shown that the conformation of the macroring parts close to the phenazine moiety in the free ligand is more similar to that in the heterochiral complex than to that which has been found in the homochiral one. This means that (*R,R*)-**1** is *preorganized* to bind (*S*)-NapEt over (*R*)-NapEt selectively;
- (v) molecular modeling also predicted the heterochiral complex to be more stable in the gas phase.

4. Experimental

4.1. General

Infrared spectra were obtained on a Zeiss Specord IR 75 spectrometer. Optical rotations were taken on a Perkin–Elmer 241 polarimeter that was calibrated by measuring the optical rotations of both enantiomers of menthol. ^1H (500 MHz) and ^{13}C (125 MHz) NMR spectra were taken on a Bruker DRX-500 Avance spectrometer. Elemental analyses were performed in the Microanalytical Laboratory of the Department of Organic Chemistry, L. Eötvös University, Budapest, Hungary. Melting points were taken on a Boetius micro melting point apparatus and were uncorrected.

X-Ray data were collected on a Rigaku R-AXIS II.C area detector using a rotating anode equipped with Mo-K α target ($\lambda=0.7071$). All structures were solved using SHELXS-86¹⁷ and refined with SHELXL-93.¹⁸

Crystal structures along with experimental details have been deposited with the CCDC.

4.2. Synthesis

(3*R*,13*R*)-(–)-Dimethyl-2,5,8,11,14-pentaoxa-20,26-diazatetracyclo[13.9.3.0.^{19,27}0^{21,25}heptacos-15,17,19,21,22,24(1),26-heptaene (*R,R*)-**1** was prepared as described in the literature.⁷ Suitable crystals of (*R,R*)-**1** for X-ray study were obtained by recrystallization from methanol. (*R*)- α -(1-Naphthyl)ethylammonium perchlorate (*R*)-NapEt and (*S*)- α -(1-naphthyl)ethylammonium perchlorate (*S*)-NapEt were prepared as reported.¹⁹

The preparation of suitable crystals for the heterochiral complex of (*R,R*)-**1**–(*S*)-NapEt was performed as follows:

Compound (*R,R*)-**1** (68 mg, 0.171 mmol) and (*S*)-NapEt (51 mg, 0.188 mmol) were refluxed in 7 mL of pure methanol until a clear solution formed. The solution was filtered while hot and it was stored at rt for 4 h, at 0°C for 1 day and at –18°C for another day. The crystals were filtered and dried in a vacuum desiccator over phosphorus pentoxide overnight to give 82 mg (72%) of yellow needles. Mp: 206–208°C. $[\alpha]_{\text{D}}^{25}=-134.9$ (*c* 0.32, CH₂Cl₂). IR (KBr) ν 3112, 3054, 2982, 2920, 2874, 1624, 1580, 1564, 1500, 1488, 1456, 1384, 1344, 1288, 1256, 1096, 996, 832, 760, 624 cm⁻¹. ^1H NMR (500 MHz, CDCl₃) δ 1.29 (broad s, 3H), 1.69 (d, *J*=7 Hz, 3H), 1.78 (broad s, 3H), 3.57–4.46 (broad m, 12H), 4.98 (broad s, 3H), 6.63 (broad s, 1H), 6.89 (broad s, 2H), 6.98 (broad s, 1H), 7.08 (t, *J*=8 Hz, 1H), 7.19 (d, *J*=8 Hz,

2H), 7.35 (d, $J=8$ Hz, 2H), 7.45–7.79 (broad m, 4H), 8.79 (broad s, 3H). ^{13}C NMR (125 MHz, CDCl_3) δ 14.69, 21.19, 45.62, 67.78, 69.85, 71.68, 74.07, 119.35, 121.75, 124.03, 125.05, 125.73, 126.08, 128.94, 129.03, 131.03, 132.45, 133.03, 133.70, 134.59, 144.51, 151.47. Anal. calcd for $\text{C}_{34}\text{H}_{40}\text{ClN}_3\text{O}_9$: C, 60.94; H, 6.02; Cl, 5.29; N, 6.27. Found: C, 60.68; H, 6.03; Cl, 5.38; N, 6.12.

Suitable crystals of the homochiral complex (*R,R*)-**1**–(*R*)-NapEt were prepared in the same way as above starting from (*R,R*)-**1** (68 mg, 0.171 mmol) and (*R*)-NapEt (51 mg, 0.188 mmol), but using only 3 mL of methanol. In this case 39 mg (34%) of yellow plates were obtained. Mp: 231–232°C. $[\alpha]_{\text{D}}^{25} = -63.8$ (c 0.32, dichloromethane). IR (KBr) ν 3116, 3075, 3032, 2984, 2920, 2877, 1625, 1580, 1560, 1488, 1456, 1376, 1344, 1280, 1252, 1096, 928, 784, 760, 624 cm^{-1} . ^1H NMR (500 MHz, CDCl_3) δ 1.26–1.72 (broad m, 6H), 1.73 (d, $J=7$ Hz, 3H), 3.52–4.48 (broad m, 12H), 4.89 (broad s, 2H), 5.24 (broad s, 1H), 6.79 (t, $J=8$ Hz, 1H), 6.92 (t, $J=8$ Hz, 1H), 7.06 (broad s, 2H), 7.14 (t, $J=8$ Hz, 1H), 7.17 (t, $J=8$ Hz, 1H), 7.23 (d, $J=8$ Hz, 1H), 7.38 (d, $J=8$ Hz, 1H), 7.48 (d, $J=8$ Hz, 1H), 7.66–7.72 (m, 4H), 8.54 (broad s, 3H). ^{13}C NMR (125 MHz, CDCl_3) δ 14.97, 20.43, 45.54, 69.03, 71.28, 73.84, 74.86, 120.98, 122.21, 123.92, 124.38, 126.02, 126.74, 128.58, 129.24, 129.61, 131.10, 132.80, 133.14, 134.27, 134.65, 144.34, 151.76. Anal. calcd for $\text{C}_{34}\text{H}_{40}\text{ClN}_3\text{O}_9$: C, 60.94; H, 6.02; Cl, 5.29; N, 6.27. Found: C, 60.69; H, 6.07; Cl, 5.16; N, 6.16.

4.3. Crystallography

Bond lengths and angles are close to the expected values in all three structures and have relatively large e.s.d.s in some cases due to the crystal quality, high thermal motion or a large degree of static disorder. The perchlorate counterions are severely disordered in both diastereomeric complexes and the disorders are not easy to resolve in a sensible manner.

Crystal data for (*R,R*)-**1**: $a=10.973(4)$ Å, $b=21.411(5)$ Å, $c=8.66(4)$ Å, $V=2034(8)$ Å³, $Z=4$, $d=1.301$ g/cm³, $\mu=0.093$ mm⁻¹, $F(000)=848$. Theta range for data collection: 1.90 to 26.45 degrees. Index ranges: $-13 \leq h \leq 13$, $-21 \leq k \leq 26$, $-9 \leq l \leq 10$. Reflections collected: 2236. Full-matrix least-squares on F^2 . Data:restraints:parameters: 2233:99:283. Goodness-of-fit on F^2 : 1.052. Final R indices [$I > 2\sigma(I)$]: $R_1=0.0652$, $wR_2=0.1667$. Final R indices [all reflections]: $R_1=0.1959$, $wR_2=0.2590$. Extinction coefficient: 0.013(4). Largest diff. peak and hole: 0.263 and -0.228 eÅ⁻³.

Crystal data for (*R,R*)-**1**–(*R*)-NapEt: $a=12.132(3)$ Å, $b=10.729(2)$ Å, $c=26.118(6)$ Å, $\beta=95.821(7)$ degrees, $V=3382(1)$ Å³, $Z=4$, $d=1.316$ g/cm³, $\mu=0.171$ mm⁻¹, $F(000)=1416$. Theta range for data collection: 1.57 to 25.97 degrees. Index ranges: $0 \leq h \leq 14$, $0 \leq k \leq 13$, $-32 \leq l \leq 31$. Reflections collected: 5979. Full-matrix least-squares on F^2 . Data:restraints:parameters: 5979:495:957. Goodness-of-fit on F^2 : 1.124. Final R indices [$I > 2\sigma(I)$]: $R_1=0.0667$, $wR_2=0.1712$. Final R indices [all reflections]: $R_1=0.0871$, $wR_2=0.1860$. Absolute structure parameter: 0.0(1). Extinction coefficient 0.007(2). Largest diff. peak and hole: 0.343 and -0.385 eÅ⁻³.

Crystal data for (*R,R*)-**1**–(*S*)-NapEt: $a=15.729(2)$ Å, $b=12.558(2)$ Å, $c=17.658(2)$ Å, $V=3488.1(8)$ Å³, $Z=4$, $d=1.310$ g/cm³, $\mu=0.170$ mm⁻¹, $F(000)=1456$. Theta range for data collection: 1.73 to 25.75 degrees. Index ranges $0 \leq h \leq 19$, $0 \leq k \leq 15$, $0 \leq l \leq 21$. Reflections collected: 3710. Full-matrix least-squares on F^2 . Data:restraints:parameters: 3708:222:483. Goodness-of-fit on F^2 : 0.858. Final R indices [$I > 2\sigma(I)$]: $R_1=0.0464$, $wR_2=0.1185$. Final R indices [all reflections]: $R_1=0.0773$, $wR_2=0.1533$. Absolute structure parameter 0.2(2). Extinction coefficient 0.016(2). Largest diff. peak and hole: 0.202 and -0.220 eÅ⁻³.

4.4. Computational studies

The LMOD calculations were carried out with a pre-release version of BatchMin 6.5²⁰ using the AMBER* force field.²¹ The electrostatic treatment of the system involved a distance dependent dielectric constant ($\epsilon=1.0$). We have found that force field charges were inadequate for these highly charged complexes. Instead, we used AM1 electrostatic potential fitted charges calculated with Spartan 4.0²² at the respective X-ray geometry of the complexes. 5000 LMOD search steps were applied for each complex and unique conformations within 30 kJ/mol above the global minimum after energy minimization were kept for the MINTA calculation. The MINTA integrals, which form the basis for the binding free energy calculation^{15,16} were evaluated as block averages using 52 000 independent, single-point energy calculations per conformation.

The combined numerical/analytical MINTA algorithm was applied with the numerical integration of the 30 lowest-frequency (soft) vibrational modes and analytical integration of the remaining (hard) modes using the harmonic approximation. Note that the soft modes per se included contributions from the relative translation and rotation of the guest with respect to the crown ether host. It should also be stressed that the LMOD/MINTA procedure was applied to unconstrained host–guest systems to make sure that both the host and the guest were fully sampled. The computations were carried out on an SGI Indy workstation.

Acknowledgements

The authors are grateful to Dr. I. Kolossvary for helpful discussions and to the Hungarian Scientific Research Fund (OTKA) (No. F019261 and T25071) for financial support.

References

1. Lehn, J. M. *Supramolecular Chemistry*; VCH: Weinheim, 1995.
2. Zang, X. X.; Bradshaw, J. S.; Izatt, R. M. *Chem. Rev.* **1997**, *97*, 3313.
3. Redd, J. T.; Bradshaw, J. S.; Huszthy, P.; Izatt, R. M.; Dalley, N. K. *J. Heterocycl. Chem.* **1998**, *35*, 1.
4. Wang, T. M.; Bradshaw, J. S.; Huszthy, P.; Kou, X.; Dalley, N. K.; Izatt, R. M. *J. Heterocycl. Chem.* **1994**, *31*, 1.
5. Izatt, R. M.; Wang, T. M.; Hathaway, J. K.; Zhang, X. X.; Curtis, J. C.; Bradshaw, J. S.; Zhu, C. Y.; Huszthy, P. *J. Incl. Phenom. Mol. Recognit. Chem.* **1994**, *17*, 157.
6. Izatt, R. M.; Zhu, C. Y.; Huszthy, P.; Bradshaw, J. S. *Crown Compounds: Toward Future Applications*; Cooper, S. R., Ed.; VCH: New York, 1992; Chapter 12.
7. Huszthy, P.; Samu, E.; Vermes, B.; Mezey-Vándor, G.; Nógrádi, M.; Bradshaw, J. S.; Izatt, R. M. *Tetrahedron* **1999**, *55*, 1491.
8. Davidson, R. B.; Bradshaw, J. S.; Jones, B. A.; Dalley, N. K.; Christensen, J. J.; Izatt, R. M. *J. Org. Chem.* **1984**, *49*, 353.
9. Davidson, R. B.; Dalley, N. K.; Izatt, R. M.; Bradshaw, J. S.; Campana, C. F. *Isr. J. Chem.* **1985**, *25*, 33.
10. Bradshaw, J. S.; Colter, M. L.; Nakatsuji, Y.; Spencer, N. O.; Brown, M. F.; Izatt, R. M.; Arena, G.; Tse, P. K.; Wilson, B. E.; Lamb, J. D.; Dalley, N. K.; Morin, F. G.; Grant, D. M. *J. Org. Chem.* **1985**, *50*, 4865.
11. Izatt, R. M.; Zhu, C. Y.; Izatt, R. M.; Bradshaw, J. S.; Dalley, N. K. *J. Incl. Phenom.* **1992**, *13*, 17.
12. Izatt, R. M.; Zhu, C. Y.; Dalley, N. K.; Curtis, J. C.; Kou, X.; Bradshaw, J. S. *J. Phys. Org. Chem.* **1992**, *5*, 656.
13. Böcskei, Zs.; Keseru, G. M.; Menyhárd, D.; Huszthy, P.; Bradshaw, J. S.; Izatt, R. M. *Acta Cryst.* **1996**, *C52*, 463.
14. Kolossváry, I.; Guida, W. C. *J. Am. Chem. Soc.* **1996**, *118*, 5011.
15. Kolossváry, I. *J. Phys. Chem. A.* **1997**, *101*, 9900.
16. Kolossváry, I. *J. Am. Chem. Soc.* **1997**, *119*, 10233.
17. Sheldrick, G. M. *Acta Cryst.* **1990**, *A46*, 467.
18. Sheldrick, G. M. *SHELXL-93, Program for the Refinement of Crystal Structures*; University of Göttingen: Germany, 1993.

19. Bradshaw, J. S.; Huszthy, P.; Wang, T. M.; Zhu, C. Y.; Nazarenko, A. Y.; Izatt, R. M. *Supramolecular Chem.* **1993**, *1*, 267.
20. Mohamadi, F.; Richards, N. G. J.; Guida, W. C.; Liskamp, R.; Lipton, M.; Caufield, C.; Chang, G.; Hendrickson, T.; Still, W. C. *J. Comput. Chem.* **1990**, *11*, 440.
21. Weiner, S. J.; Kollman, P. A.; Case, D. A.; Singh, U. C.; Ghio, C.; Alagona, G.; Profeta Jr., S.; Weiner, P. *J. Am. Chem. Soc.* **1984**, *106*, 765.
22. SPARTAN, 1994, V4.0, Wavefunction Inc. 18401 Von Karman Ave #370, Irvine, 92715, USA.